J Pharmacol Sci **106**, 287 – 294 (2008)

*Journal of Pharmacological Sciences*


*Full Paper*

# Caveolae/Caveolin-1 Are Important Modulators of Store-Operated Calcium Entry in Hs578/T Breast Cancer Cells

Hua Zhu[1,*], Noah Weisleder[2], Ping Wu[3], Chuanxi Cai[2], and Jian-wen Chen[3]

[1]*The Cancer Institute of New Jersey,* [2]*Department of Physiology and Biophysics, University of Medicine and Dentistry of New Jersey, New Brunswick, NJ 08901, USA*
[3]*Center of Systems Biology, Institute of Biophysics, Chinese Academy of Sciences, Beijing 100101, China*

*Received July 24, 2007; Accepted December 19, 2007*

**Abstract.** Caveolin-1 is a principal component of caveolae, invaginations of the plasma membrane that are enriched in cholesterol and sphingolipids. The expression of caveolin-1 has been shown to be tightly correlated to the progression of breast cancer tumors. However, the consequences of altered caveolin-1 expression during tumor progression still remain unclear. Modification of caveolin-1 expression modulates store-operated $Ca^{2+}$ entry (SOCE) in various cell types. SOCE is a ubiquitous $Ca^{2+}$ entry pathway that previous studies have linked to apoptosis and tumor progression in prostate cancer cells. In this study, we tested the effect of altering caveolin-1 expression on SOCE in Hs578/T breast cancer cells. Through overexpression of caveolin-1 and small hairpin RNA (shRNA) knockdown, we generated four stable cell lines that have 3 different caveolin-1 protein levels. Cav-1 overexpression could increase SOCE activity, while knockdown of caveolin-1 significantly reduced SOCE activity. These functional consequences were correlated with changes in caveolae number in Hs578/T cells. Our results suggest alteration of SOCE by caveolin-1 expression changes could be one of the mechanisms contributing to the progression of breast cancer.

***Keywords***: caveolae, caveolin-1, store-operated calcium channel, tumor progression

## Introduction

Caveolae are vesicular membrane structures that are found in plasma membranes of many cell types (1, 2). Caveolin-1, a major protein component of caveolae, has been linked to numerous physiological and pathophysiological processes since its discovery over a decade ago. In addition to the well-known functions of caveolin-1 in signal transduction (3), cholesterol homeostasis (4), and vesicular transport (5), it also has both tumor suppressor and oncogenic functions. Recent work from other investigators showed that caveolin expression is altered in a stage-dependent manner during cancer development [see reviews (6, 7) for detailed information]. In the early stages of carcinogenesis, decreased caveolin-1 expression leads to rapid, unregulated cell growth. In the later cancer stages, caveolin-1 expression increases to render cells more resistant to cell death and progress towards an invasive phenotype. While this association between caveolin-1 expression and tumor progression has been established, the molecular mechanism by which caveolin expression could contribute to tumorgenesis is less defined.

From other studies, we also know caveolae are sites of $Ca^{2+}$ entry into the cell. Following depletion of the $Ca^{2+}$ stored within the endoplasmic reticulum (ER), caveolae are the preferred sites of $Ca^{2+}$ entry (8 – 10). This store-operated $Ca^{2+}$ entry (SOCE) mechanism can refill $Ca^{2+}$ stores to maintain intracellular $Ca^{2+}$ signaling and homeostasis. Aside from this essential physiological function, SOCE has been implicated in apoptosis and tumor progression. Previous studies in prostate cancer cells demonstrated that ER stress–induced apoptosis is due to reduced SOCE (11 – 13). SOCE is also required for cancer proliferation (14), invasion, and metastasis (15).

Other studies indicate a molecular basis for caveolin-1 function in SOCE activation. Several members of the

*Corresponding author. Zhuhu2@umdnj.edu
Published online in J-STAGE
doi: 10.1254/jphs.FP0071192

transient receptor potential (TRP) family of putative store-operated $Ca^{2+}$ channels (SOC) are enriched in caveolae (16 – 18). Caveolin-1 was reported to bind the N terminus of TRPC1, one of the TRP family proteins, to assist in activation of SOCE (16, 19). Recently it was found that a $Ca^{2+}$-binding sensor protein, stromal interaction molecule 1 (STIM1), plays a key role in SOCE activation (20, 21). Like caveolin-1, it can also bind and activate TRPC1 (22). Additionally, caveolin-1 and STIM1 expression are co-regulated in osteosarcoma cells (23).

Considering the available evidence, we hypothesize that differential expression of caveolin-1 can regulate the SOCE in breast cancer cells. In the present study, we tested this hypothesis by measuring the different rates of SOCE in stable cell lines that express different levels of caveolin-1. The cells that express additional caveolin-1 display elevated SOCE activity, while SOCE activity is depressed in cells with reduced caveolin-1 expression. Through pharmacological manipulation, as well as electron and confocal microscopy, we confirmed that caveolin-1 could specifically influence SOCE activity by mediating caveolae formation. Our results suggest that caveolae/caveolin-1 may play a role in tumor progression by regulating SOCE activity and also indicate that the stable Hs578/T cell line with altered caveolin-1 expression may be an effective model for considering the role of SOCE modification in breast cancer carcinogenesis.

## Materials and Methods

*Materials*

The monoclonal antibody (mAb) (Z034) against caveolin-1 was purchased from Zymed Laboratories, Inc. (South San Francisco, CA, USA). Mouse monoclonal anti-$\beta$-actin (AC-74) was purchased from Sigma (St. Louis, MO, USA). Texas Red-labeled goat anti-mouse IgG was purchased from Invitrogen-Molecular Probes, Inc. (Eugene, OR, USA). Cell culture supplies (RPMI 1640 medium, geneticin, fetal bovine serum, L-glutamine, trypsin-EDTA, Lipofectamine 2000, and penicillin/streptomycin) were all from Invitrogen-Life Technologies, Inc. (Carlsbad, CA, USA). BCIP/NBT reagents were purchased from Promega (Madison, WI, USA). The pCI-neo and pCI-neo-cav-1 plasmids were generous gifts from Dr. Eric J. Smart (Kentucky Medical School, Kentucky, USA). Four plasmids (pBCMGneo-Sequence-1, pBCMGneo-Sequence-2, pBCMGneo-Shuffle-1, or pBCMGneo-Shuffle-2) were generous gifts from Dr. K. Liao (Institute of Biochemistry and Cell Biology, Shanghai Institutes for Biological Sciences, Chinese Academy of Sciences, Shanghai, 200031, China). Fura-2-AM, methyl-$\beta$-cyclodextrin (M$\beta$CD), thapsigargin (TG), 2-aminoethoxydiphenyl borate (2-APB), and SKF-96365 were purchased from Sigma and prepared in dimethyl sulfoxide (DMSO) as stock solutions. For experiments using these compounds, equivalent volumes of DMSO were added to control cells prior to experimentation. All other reagents were obtained from regular commercial sources at the highest available purity.

*Cell lines, plasmids, and transfections*

The parental human breast cancer cell line Hs578/T was a generous gift from Dr. Kjell Grankvist (Umea University, Sweden) (24) . The cells were cultured at 37°C, 5% $CO_2$ in RPMI 1640 medium supplemented with 10% fetal bovine serum, 2 mM glutamine, 100 units/ml penicillin, and 100 $\mu$g/ml streptomycin. The entire cDNA sequence of caveolin-1 (Genbank #BC009685) was cloned into the EcoRI site of pCI-neo to generate pCI-neo-cav-1. PCI-neo-cav-1 and PCI-neo (empty vector) were transfected into Hs578T cell lines to overexpress caveolin-1 as described (25). Four plasmids were used for generation of stable cell lines expressing small hairpin RNA (shRNA) to target caveolin-1 for RNA interference knockdown. These four plasmids (pBCMGneo-Sequence-1, pBCMGneo-Sequence-2, pBCMGneo-Shuffle-1, or pBCMGneo-Shuffle-2) were transfected into Hs578/T cell lines to knock down caveolin-1 expression as described (26). After screening for the degree of caveolin-1 protein knockdown, a stable line generated from pBCMGneo-Sequence-2 was used in functional studies.

*Western blotting*

Proteins were separated by SDS-PAGE with a standard reducing condition protocol as described (27). Samples were resuspended in a sample buffer and loaded on 12% acrylamide-bisacrylamide gels. After electrophoresis, proteins were transferred to a nitrocellulose membrane. Blots were blocked by 5% nonfat dry milk, 0.05% Tween 20 in Tris-buffered saline (10 mM Tris, pH 8.0, 135 mM NaCl). Immunoblotting was performed with the designated antibodies and detection was performed with the BCIP/NBT reagents according to the manufacturer's instructions.

*Measurement of SOCE by $Mn^{2+}$ quenching of fura-2 fluorescence*

Cells were loaded with fura-2-AM (2 $\mu$M) for 30 min in a balanced salt solution (BSS: 140 mM NaCl, 2.8 mM KCl, 2 mM $CaCl_2$, 2 mM $MgCl_2$, 10 mM HEPES, pH 7.2) at room temperature. After loading, cells were washed 3 times with loading buffer without fura-2-AM

and then incubated for an additional 30 min at room temperature to complete ester hydrolysis. Fura-2 was excited at 340 and 380 nm for determinations of $[Ca^{2+}]_i$ and at the isosbestic wavelength of 360 nm for determining $Mn^{2+}$ quenching. The recording was conducted on an inverted microscope (Axiovert S100 TV; Zeiss, Germany) equipped with a polychromatic Xenon light source (TILL Photonics, Gräfeling, Germany) at room temperature. Emitted light was collected with a photodiode controlled by the TILL photometry system (TILL Photonics) and X-Chart extension of the Pulse software.

Intracellular concentration of $Ca^{2+}$ was determined as described by Grynkiewicz et al. (28). The release of intracellular $Ca^{2+}$ in individual cells was measured following exposure to thapsigargin in a $Ca^{2+}$-free BSS solution (plus 0.5 mM EGTA) by rapid solution exchange perfusion. Data were analyzed using Igor software (version 4.0.3.0) and background fluorescence was subtracted to establish the final values.

Quenching of Fura-2 fluorescence at an excitation wavelength of 360 nm (F360) was used to assay SOCE activity in individual cells as described (29). $Mn^{2+}$ can enter the cell via SOCE but cannot be exported by the plasma membrane $Ca^{2+}$ ATPase (30) or by $Na^+/Ca^{2+}$ exchange (31). Once inside the cell, $Mn^{2+}$ can bind fura-2 and reduce the fluorescence of the dye. In trials to measure maximal SOCE activation, the ER $Ca^{2+}$ store of fura-2-loaded cells was depleted by TG, 0.5 mM $Mn^{2+}$ was then added, and the decline of F360 ($Mn^{2+}$ quench) was observed. For trials to examine the graded activation of SOCE, $Mn^{2+}$ was added first and then TG was added to induce SOCE. Linear fits using least-squares regression analysis were performed 30 s before and 30 s after an observed decrease in the 360 nm quench rate. At the conclusion of the trial, Triton X-100 was added to lyse the cells and the resulting rapid decline in the fluorescence was used as the minimal value (with the pre-quenching fluorescence as the maximal value) to normalize the results to 1.

*Transmission electron microscopy*

Samples were fixed with glutaraldehyde, post-fixed with osmium tetroxide, and stained with uranyl acetate and lead citrate, as described (32). Samples were examined with a Philips Technai 20 TEM (Philips, Eindhoven, The Netherlands).

*Immunostaining*

Cells were cultured on a cover glass and then stained using previously described protocols (33). Briefly, cells were fixed in phosphate-buffered saline (PBS) containing 4% paraformaldehyde at room temperature for 20 min. Fixed cells were rinsed with PBS and treated with 25 mM $NH_4Cl$ in PBS for 10 min to quench free aldehyde groups. The cells were permeabilized by incubation for 15 min in freshly-prepared 0.1% Triton X-100/PBS. The cells were preincubated for 1 h in PBS containing 5% normal goat serum and then incubated for 2 h in diluted caveolin-1 (1:100) antibody in PBS containing 2.5% goat serum. Washing of the coverslip three times was followed by incubation for 1 h in 1:200-diluted Texas Red–labeled goat anti-mouse IgG. After extensive PBS washes, immunostained cells were examined with a Bio-Rad Radiant-2100 confocal microscope (Bio-Rad, Hercules, CA, USA). More than 100 cells were inspected per experiment, and the results displayed are typical.

*Statistical analyses*

Group data are presented as the mean ± S.E.M. Analysis of statistical significance was conducted using one-way ANOVA followed by Bonferroni's test.

## Results

*Establishing stable Hs578/T cell lines with altered caveolin-1 expression*

Hs578/T cells were transfected with PCI + neo-caveolin-1 or PCI + neo-vector plasmids to generate stable clones that overexpressed caveolin-1 [Cav(+)] or contained the vector plasmid as a control (vector). We also transfected two pairs of shRNA plasmids (pBCMGneo-Sequence-1, pBCMGneo-Sequence-2, pBCMGneo-Shuffle-1, or pBCMGneo-Shuffle-2) into Hs578/T cells to generate stable cell lines. We found the Sequence-2 probe was more effective at reducing caveolin-1 expression than Sequence-1, so our experiments used a stable cell line from the Sequence-2–transfected cells [Cav(–)] and a corresponding shuffle-2 control cell line (Shuffle).


**Fig. 1.** Differential expression of caveolin-1 in four stable H578/T stable cell lines. Upper panel shows caveolin-1 expression, and the lower panel shows the *β*-actin content as a control for loading.

Caveolin-1 was overexpressed approximately 6-fold in Cav(+) cells compared to Vector cells (Fig. 1: upper panel, lanes 3 and 4). Expression of caveolin-1 was almost completely blocked in Cav(−) cells (Fig. 1: upper panel, lanes 1 and 2). As expected, caveolin-1 protein levels in Vector and Shuffle cells are the same. Our studies presented here were conducted with these four stable cell lines expressing 3 different caveolin-1 protein levels.

*Caveolin-1 regulates SOCE activity*

To determine if modulating caveolin-1 expression alters SOCE in breast cancer cells we performed $Mn^{2+}$-quenching experiments in these four cell lines. In this assay, $Mn^{2+}$ is provided outside of the cell to act as a surrogate for $Ca^{2+}$ during SOCE. As $Mn^{2+}$ quenches fura-2 fluorescence, this provides a method of determining SOCE activity. While this is a widely used method for measuring SOCE, our results using the $Mn^{2+}$ quenching assay were confirmed by measurement of $Ca^{2+}$ entry (data not shown).

Intracellular $Ca^{2+}$ stores were depleted by TG in the absence of external $Ca^{2+}$, and then $Mn^{2+}$ was added to the medium and the quenching rates monitored. Representative traces of fura-2 fluorescence illustrate that SOCE activity in caveolin-1 overexpressing cells is higher than vector control cells and scrambled shRNA cells, and SOCE is repressed in caveolin-1 shRNA cells (Fig. 2A). To quantitate the rate of SOCE, we computed the initial slopes of the decay of fluorescence following $Mn^{2+}$ addition (Fig. 2C). By determining these measurements, we established that the rate of SOCE in Cav(+) cells is about 2.5- and 5-fold higher than that in Vector or Cav(−) cells, respectively (Fig. 2C).

To confirm that caveolin-1 overexpression directly induces SOCE, we subjected Cav(+) and Vector cells to preincubation with 5 mM M$\beta$CD, which disrupts caveolae by depleting cholesterol, for 30 min before SOCE measurements. Following M$\beta$CD treatment, the elevated SOCE in Cav(+) returned to the level of untreated Vector control cells (Fig. 2: B and C). This suggests that caveolin-1 expression alters SOCE by affecting caveolae structures on the plasma membrane, although there are other potential effects of M$\beta$CD treatment.

*$Ca^{2+}$ entry in Hs578/T cells is blocked by SOCE inhibitors*

While the use of TG to trigger ER store depletion should specifically induce SOCE, we used the available pharmacological inhibitors of SOCE to confirm the nature of the $Ca^{2+}$ entry we observed in Hs578/T cells. To this end, we investigated the ability of the lanthanide

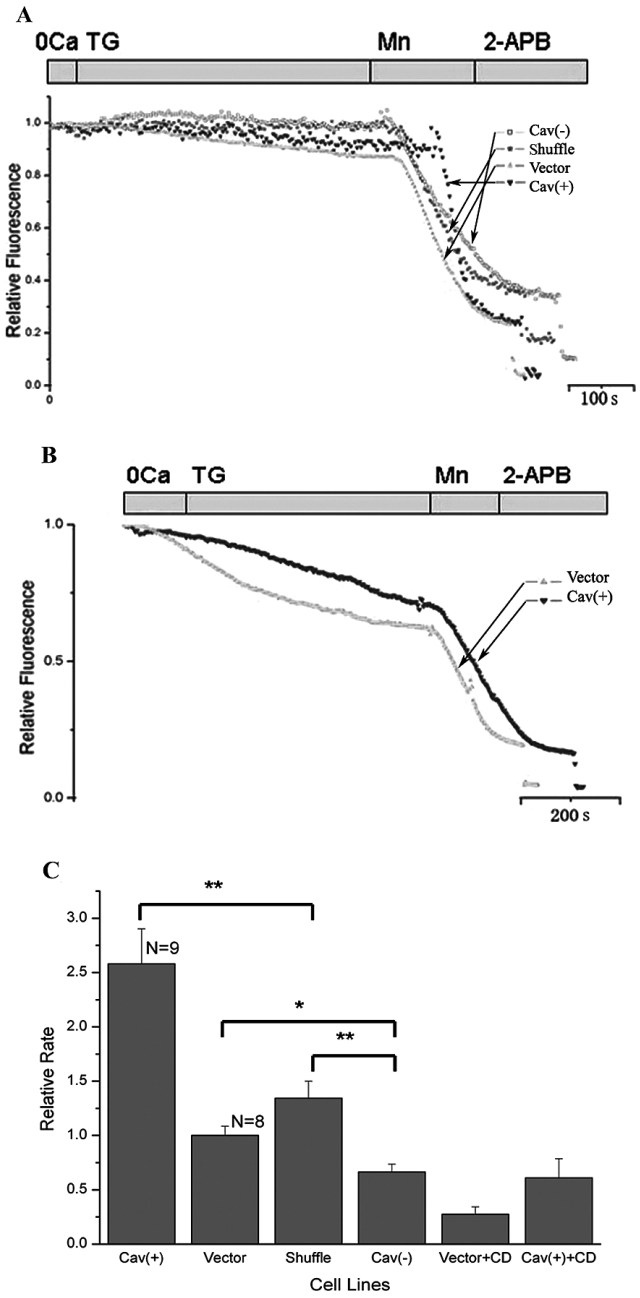


**Fig. 2.** SOCE is modified by altering caveolin-1 expression in Hs578/T cell lines. A: Representative traces of fura-2 fluorescence at $F_{360}$ illustrate the quenching of fura-2 fluorescence by $Mn^{2+}$ entry after TG-induced ER $Ca^{2+}$ depletion in Cav(−), Shuffle, Vector, and Cav(+) cells. After about 100 s, a SOCE inhibitor (2-APB, SKF-96365, or $Gd^{3+}$) was added to block the channel. This figure shows the inhibition by 2-APB. The other two inhibitors have similar effects (data not shown). Triton X-100 (0.1%) was added to permeabilize the cell membrane at the end of the experiment. B: Cells were preincubated with M$\beta$CD (5 mM, 30 min, 37°C), and then the quenching rate was measured. C: Changes in the rate of Fura-2 quenching by $Mn^{2+}$ expressed as relative changes in fluorescence per unit time and averaged from multiple experiments. The quenching rate of Vector cells was set to 1. Data from multiple experiments are presented as means ± S.E.M. Data were obtained from six individual experiments. *$P$<0.05, **$P$<0.01.

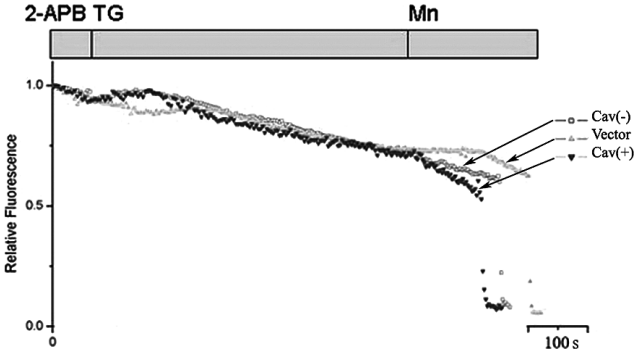


**Fig. 3.** SOCE can be specifically activated in Hs578/T cells. Cells were preincubated with an SOCE inhibitor, 2-APB, and then SOCE was measured by $Mn^{2+}$ quenching. 2-APB could almost totally block ion entry in cav(+), cav(−), and Vector cells. Other SOCE inhibitors, SKF96365 and $Gd^{3+}$, were also applied and produced similar results.

ion gadolinium ($Gd^{3+}$) (34), which is a non-specific $Ca^{2+}$-channel blocker, as well as SKF-96365 (35) and 2-APB (36), blockers of SOCE, to inhibit $Ca^{2+}$ entry. Then we used TG to deplete intracellular $Ca^{2+}$ stores in the absence of external $Ca^{2+}$ and in presence of either 250 $\mu$M $Gd^{3+}$, 25 $\mu$M SKF-96365, or 20 $\mu$M 2-APB. Multiple inhibitors were used in these experiments to limit the potential off-target effects of these inhibitors on our experimental results. While the initial intracellular $Ca^{2+}$ increase in response to TG was unaffected by these compounds (data not shown), the quenching of fura-2 fluorescence following $Mn^{2+}$ addition in Cav(−), Vector, and Cav(+) cells was completely blocked by all three inhibitors (Figs. 2B, 2C, and 3). This data confirms that the effects on $Ca^{2+}$ entry induced by altering caveolin-1 expression are the result of modification of SOCE activity.

*Altered caveloin-1 expression affects the graded activation of SOCE in Hs578/T cells*

Our results indicate that the maximal rate of SOCE activation is altered in the Hs578/T breast cancer cells with various levels of caveolin-1 expression (Fig. 2). A unique characteristic of SOCE is its graded activation in response to ER $Ca^{2+}$ store depletion. To examine the effect of altered caveolin-1 expression on the graded activation of SOCE, we modified our procedure to initially provide $Mn^{2+}$ in $Ca^{2+}$-free BSS solution and monitored the fluorescence intensity to establish the basal $Mn^{2+}$ entry (curve a in Fig. 4A). We then used TG to deplete the $Ca^{2+}$ stores and activate SOCE. Monitoring the resulting decrease in fura-2 fluorescence allows determination of the slope of the decay curve (curve b in Fig. 4A). The dynamic $Mn^{2+}$ quenching rate is calculated as the ratio of a and b (b/a). We found that the graded activation rate of SOCE was altered with different levels

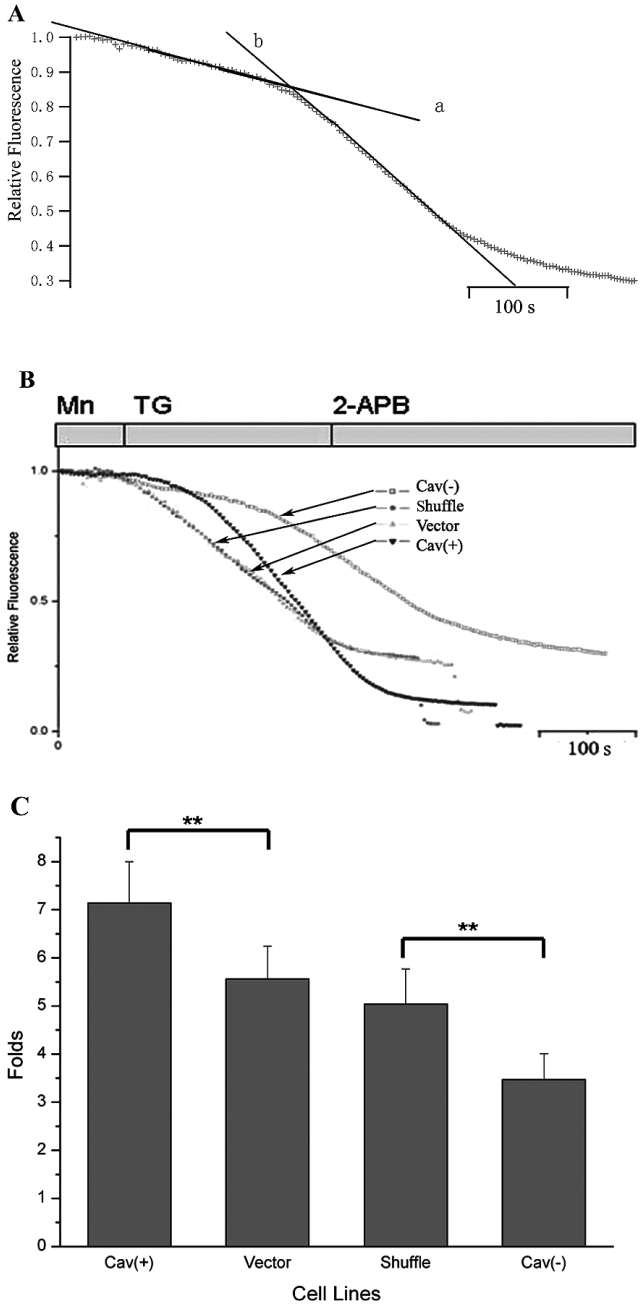


**Fig. 4.** Caveolin-1 expression can modify the activation of SOCE. A: Addition of TG after $Mn^{2+}$ induces a sigmoidal quenching curve due to the graded activation of SOCE following initial store depletion. The quenching rate is the ratio (b/a) of the linear fit for the basal entry rate (a) and a linear fit of the initial phase of the quenching curve (b). B: Quenching of fura-2 fluorescence by preincubated $Mn^{2+}$ in the four cell lines followed by TG-induced ER $Ca^{2+}$ depletion. C: The calculated quenching rate for each of the four cell lines. Data from multiple experiments are presented as means ± S.E.M. Data were obtained from six individual experiments. $^{**}P<0.01$.

of caveolin-1 expression (Fig. 4B). Cav(+) cells display accelerated SOCE activation, and SOCE activation is slowed in Cav(−) cells (Fig. 4C), mirroring the effect of

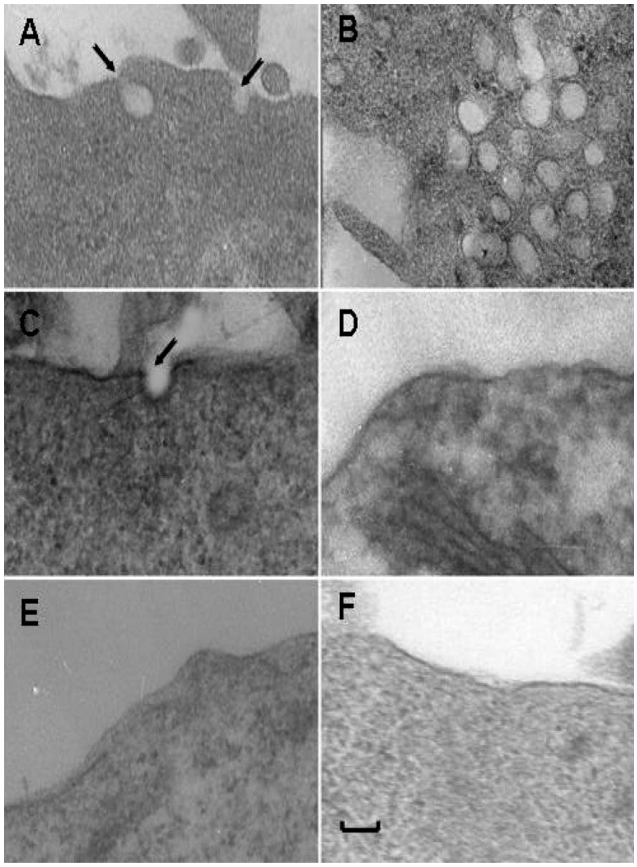


**Fig. 5.** Visualization of caveolae in Hs578/T cells by electron microscopy. Each panel shows representative EM micrographs of caveolae on the plasma membrane of various cell lines. Caveolae are indicated by arrowheads. A: Vector, B: Cav(+), C: Shuffle, D: Cav(−), E: Vector + M$\beta$CD, F: Cav(+) + M$\beta$CD. Bar = 100 nm.

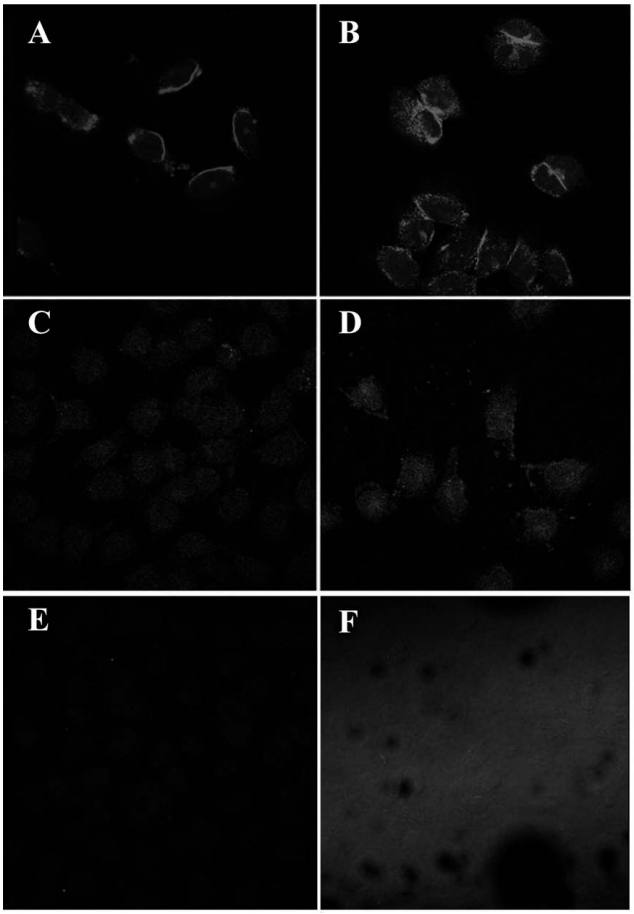


**Fig. 6.** Relocation of caveolin-1 from caveolae after M$\beta$CD treatment. Immunofluorescence was used to determine the subcellular location of caveolin-1. A: Vector cells, B: Cav(+) cells, C: Vector cells after M$\beta$CD treatment, D: Cav(+) cells after M$\beta$CD treatment, E: Cav(−), F: transmission microphotograph (bright field) of E to indicate the location of cells.

caveolin-1 expression on the maximal rate of SOCE activation.

*Caveolin-1–mediated caveolae formation is associated with SOCE*

Caveolin-1 is an essential component for the formation of caveolae at the plasma membrane. As caveolae are important sites of $Ca^{2+}$ entry, we tested if modulation of caveolin-1 expression would alter the formation of caveolae while also affecting SOCE. We observed each cell line by electronic microscopy (EM) and found the number of caveolae present is dependent on the caveolin-1 expression level (Fig. 5). As a control for the effectiveness of M$\beta$CD treatment in our SOCE studies, we applied the same conditions to cells before fixation for EM. These conditions effectively reduce the formation of caveolae, both in Vector cells and in Cav(+) cells (Fig. 5: E and F), indicating that altered caveolae number is a key to SOCE regulation in Hs578/T breast cancer cells.

used confocal microscopy to determine the location of caveolin-1 before and after M$\beta$CD treatment (Fig. 6). We found a higher level of caveolin-1 protein at the plasma membrane in the Cav(+) cells (Fig. 6B) than in Vector cells (Fig. 6A). No detectable caveolin-1 protein can be observed in Cav(−) cells (Fig. 6E). After M$\beta$CD treatment, caveolin-1 relocates from the plasma membrane to the cytoplasm (Fig. 6: C and D), confirming that these conditions are effective at disrupting caveolin-1 localization to caveolae structures.

## Discussion

There is a growing body of evidence that caveolae are important $Ca^{2+}$ entry sites on the cell membrane. SOCE can be mediated through these sites, and the role of SOCE in tumorgenesis is now coming under more intensive study. To gain insight into whether caveolae

/caveolin-1 plays a role in the SOCE in breast cancer cells, we selected Hs578/T breast cancer cells that were stably transfected with caveolin-1 cDNA or shRNA. In our studies presented here, we found the expression level of caveolin-1 closely correlates with the activity of SOCE. Overexpression of caveolin-1 increased the activation and maximal rate of SOCE, while decreased caveolin-1 expression inhibited SOCE activation and activity. We confirmed the specificity of SOCE in these cells using 2-APB and SKF96365. While these inhibitors show non-specific effects other than inhibiting SOCE, we used a concentration that should effectively avoid off-target effects. In any case, the use of two inhibitors should help minimize concerns about off-target effects.

Our studies link modulation of SOCE by caveolin-1 with the formation of caveolae on the plasma membrane. By using M$\beta$CD to disrupt the caveolae structure, we found that SOCE activity in Cav(+) and Vector cells decreased to the level in Cav(−) cells. Using EM, only a minimal number of caveolae can be resolved on the membrane of Cav(−) cells and M$\beta$CD-treated cells. M$\beta$CD treatment may produce additional off-target effects, but nonetheless, the combination of the EM results and the effects of modulating caveolin-1 expression on SOCE activity provide strong evidence that caveolae formation mediated by caveolin-1 is an important component of SOCE activation in breast cancer cells.

Recently, additional studies have linked changes in caveolin-1 expression to tumor progression (6, 7). Our findings indicate that one mechanism by which caveolin-1 expression could affect cancer progression is by modulating SOCE activity, as SOCE is known to regulate tumor proliferation and progression in cancer cells (1 – 5). We hypothesize that cancer cells may regulate SOCE activity by altering caveolin-1 expression during different stages of tumor progression. In early stages, decreased caveolin-1 expression could lower SOCE activity to prevent apoptosis and allow for proliferation. After tumor formation, caveolin-1 expression could increase to stimulate intracellular $Ca^{2+}$ signaling to facilitate metastasis.

The molecular mechanism that mediates caveolin-1 modulation of SOCE should be a target for future investigations. Several $Ca^{2+}$-handling molecules appear to be co-localized with or associated with caveolin-1 using immunohistochemistry. These include a form of $IP_3R$ (37), the plasma membrane $Ca^{2+}$ pump (PMCA) (38), sodium $Ca^{2+}$ exchanger (NCX1) (39), an isoform of nNOS (40), and members of the transient receptor potential (TRP) family (16 – 18). It is possible that caveolin-1 interacts with TRPC1, which can then interact with STIM1 on the ER membrane. Another possibility for caveolin-1 function in SOCE regulation would be to act as a molecular scaffold domain that provides a structural context to allow efficient function of the $Ca^{2+}$-handling proteins located in caveolae (41).

In summary, we found the level of caveolin-1 expression closely correlates with the activity of SOCE in a breast cancer cell line. By EM and confocal microscopy, we found caveolin-1–mediated formation of caveolae can regulate the activity of SOCE. Our observations indicate caveolin-1 expression can modulate SOCE in breast cancer cells, suggesting that this regulation may play a role in tumorgenesis.

## Acknowledgments

This work was supported by the Natural Science Foundation of China (30030186 and 30230120). We thank Drs. Eric J. Smart (Kentucky Medical School, Kentucky, USA), K. Liao (Institute of Biochemistry and Cell Biology, Shanghai Institutes for Biological Sciences, Chinese Academy of Sciences, China), and Kjell Grankvist (Umea University, Sweden) for providing the valuable reagents and cell line, Dr. Jianjie Ma (University of Medicine and Dentistry of New Jersey, New Jersey, USA) for advice and comments, and Dr. Brad R. Evans (The Cancer Institute of New Jersey, New Jersey, USA) for comments on the manuscript.

## References

1 Anderson RG. The caveolae membrane system. Annu Rev Biochem. 1998;67:199–225.
2 Yamada E. The fine structure of the gall bladder epithelium of the mouse. J Biophys Biochem Cytol. 1955;1:445–458.
3 Smart EJ, Graf GA, McNiven MA, Sessa WC, Engelman JA, Scherer PE, et al. Caveolins, liquid-ordered domains, and signal transduction. Mol Cell Biol. 1999;19:7289–7304.
4 Pike LJ, Han X, Chung KN, Gross RW. Lipid rafts are enriched in arachidonic acid and plasmenylethanolamine and their composition is independent of caveolin-1 expression: a quantitative electrospray ionization/mass spectrometric analysis. Biochemistry. 2002;41:2075–2088.
5 Orlandi PA, Fishman PH. Filipin-dependent inhibition of cholera toxin: evidence for toxin internalization and activation through caveolae-like domains. J Cell Biol. 1998;141:905–915.
6 Carver LA, Schnitzer JE. Caveolae: mining little caves for new cancer targets. Nature reviews. 2003;3:571–581.
7 Bouras T, Lisanti MP, Pestell RG. Caveolin-1 in breast cancer. Cancer biology & therapy. 2004;3:931–941.
8 Isshiki M, Anderson RG. Function of caveolae in Ca2+ entry and Ca2+-dependent signal transduction. Traffic. 2003;4:717–723.
9 Isshiki M, Ando J, Yamamoto K, Fujita T, Ying Y, Anderson RG. Sites of Ca(2+) wave initiation move with caveolae to the trailing edge of migrating cells. J Cell Sci. 2002;115:475–484.
10 Isshiki M, Ying YS, Fujita T, Anderson RG. A molecular sensor

detects signal transduction from caveolae in living cells. J Biol Chem. 2002;277:43389–43398.
11 Vanden Abeele F, Skryma R, Shuba Y, Van Coppenolle F, Slomianny C, Roudbaraki M, et al. Bcl-2-dependent modulation of Ca(2+) homeostasis and store-operated channels in prostate cancer cells. Cancer cell. 2002;1:169–179.
12 Prevarskaya N, Skryma R, Shuba Y. Ca2+ homeostasis in apoptotic resistance of prostate cancer cells. Biochem Biophys Res Commun. 2004;322:1326–1335.
13 Vanoverberghe K, Vanden Abeele F, Mariot P, Lepage G, Roudbaraki M, Bonnal JL, et al. Ca2+ homeostasis and apoptotic resistance of neuroendocrine-differentiated prostate cancer cells. Cell Death Differ. 2004;11:321–330.
14 Weiss H, Amberger A, Widschwendter M, Margreiter R, Ofner D, Dietl P. Inhibition of store-operated calcium entry contributes to the anti-proliferative effect of non-steroidal anti-inflammatory drugs in human colon cancer cells. Int J Cancer. 2001;92:877–882.
15 Jiang JL, Zhou Q, Yu MK, Ho LS, Chen ZN, Chan HC. The involvement of HAb18G/CD147 in regulation of store-operated calcium entry and metastasis of human hepatoma cells. J Biol Chem. 2001;276:46870–46877.
16 Lockwich TP, Liu X, Singh BB, Jadlowiec J, Weiland S, Ambudkar IS. Assembly of Trp1 in a signaling complex associated with caveolin-scaffolding lipid raft domains. J Biol Chem. 2000;275:11934–11942.
17 Torihashi S, Fujimoto T, Trost C, Nakayama S. Calcium oscillation linked to pacemaking of interstitial cells of Cajal: requirement of calcium influx and localization of TRP4 in caveolae. J Biol Chem. 2002;277:19191–19197.
18 Trevino CL, Serrano CJ, Beltran C, Felix R, Darszon A. Identification of mouse trp homologs and lipid rafts from spermatogenic cells and sperm. FEBS Lett. 2001;509:119–125.
19 Brazer SC, Singh BB, Liu X, Swaim W, Ambudkar IS. Caveolin-1 contributes to assembly of store-operated Ca2+ influx channels by regulating plasma membrane localization of TRPC1. J Biol Chem. 2003;278:27208–27215.
20 Liou J, Kim ML, Heo WD, Jones JT, Myers JW, Ferrell JE Jr, et al. STIM is a Ca2+ sensor essential for Ca2+-store-depletion-triggered Ca2+ influx. Curr Biol. 2005;15:1235–1241.
21 Roos J, DiGregorio PJ, Yeromin AV, Ohlsen K, Lioudyno M, Zhang S, et al. STIM1, an essential and conserved component of store-operated Ca2+ channel function. J Cell Biol. 2005;169:435–445.
22 Huang GN, Zeng W, Kim JY, Yuan JP, Han L, Muallem S, et al. STIM1 carboxyl-terminus activates native SOC, I(crac) and TRPC1 channels. Nat Cell Biol. 2006;8:1003–1010.
23 Wang L, Takaku S, Wang P, Hu D, Hyuga S, Sato T, et al. Ganglioside GD1a regulation of caveolin-1 and Stim1 expression in mouse FBJ cells: augmented expression of caveolin-1 and Stim1 in cells with increased GD1a content. Glycoconj J. 2006;23:303–315.
24 Jonsson O, Behnam-Motlagh P, Persson M, Henriksson R, Grankvist K. Increase in doxorubicin cytotoxicity by carvedilol inhibition of P-glycoprotein activity. Biochem Pharmacol. 1999;58:1801–1806.
25 Uittenbogaard A, Smart EJ. Palmitoylation of caveolin-1 is required for cholesterol binding, chaperone complex formation, and rapid transport of cholesterol to caveolae. J Biol Chem. 2000;275:25595–25599.
26 Hong S, Huo H, Xu J, Liao K. Insulin-like growth factor-1 receptor signaling in 3T3-L1 adipocyte differentiation requires lipid rafts but not caveolae. Cell Death Differ. 2004;11:714–723.
27 Zhu H, Cai C, Chen J. Suppression of P-glycoprotein gene expression in Hs578T/Dox by the overexpression of caveolin-1. FEBS Lett. 2004;576:369–374.
28 Grynkiewicz G, Poenie M, Tsien RY. A new generation of Ca2+ indicators with greatly improved fluorescence properties. J Biol Chem. 1985;260:3440–3450.
29 Hallam TJ, Jacob R, Merritt JE. Evidence that agonists stimulate bivalent-cation influx into human endothelial cells. Biochem J. 1988;255:179–184.
30 Enyedi A, Sarkadi B, Nyers A, Gardos G. Effects of divalent metal ions on the calcium pump and membrane phosphorylation in human red cells. Biochim Biophys Acta. 1982;690:41–49.
31 Allen TJ. The effects of manganese and changes in internal calcium on Na-Ca exchange fluxes in the intact squid giant axon. Biochim Biophys Acta. 1990;1030:101–110.
32 Lavie Y, Fiucci G, Liscovitch M. Up-regulation of caveolae and caveolar constituents in multidrug-resistant cancer cells. J Biol Chem. 1998;273:32380–32383.
33 Li S, Couet J, Lisanti MP. Src tyrosine kinases, Galpha subunits, and H-Ras share a common membrane-anchored scaffolding protein, caveolin. Caveolin binding negatively regulates the auto-activation of Src tyrosine kinases. J Biol Chem. 1996;271:29182–29190.
34 Hescheler J, Schultz G. Nonselective cation channels: physiological and pharmacological modulations of channel activity. EXS. 1993;66:27–43.
35 Merritt JE, Armstrong WP, Benham CD, Hallam TJ, Jacob R, Jaxa-Chamiec A, et al. SK&F 96365, a novel inhibitor of receptor-mediated calcium entry. J Biol Chem. 1990;271:515–522.
36 Bootman MD, Collins TJ, Mackenzie L, Roderick HL, Berridge MJ, Peppiatt CM. 2-aminoethoxydiphenyl borate (2-APB) is a reliable blocker of store-operated Ca2+ entry but an inconsistent inhibitor of InsP3-induced Ca2+ release. FASEB J. 2002;16:1145–1150.
37 Fujimoto T, Nakade S, Miyawaki A, Mikoshiba K, Ogawa K. Localization of inositol 1,4,5-trisphosphate receptor-like protein in plasmalemmal caveolae. J Cell Biol. 1992;119:1507–1513.
38 Fujimoto T. Calcium pump of the plasma membrane is localized in caveolae. J Cell Biol. 1993;120:1147–1157.
39 Teubl M, Groschner K, Kohlwein SD, Mayer B, Schmidt K. Na(+)/Ca(2+) exchange facilitates Ca(2+)-dependent activation of endothelial nitric-oxide synthase. J Biol Chem. 1999;274:29529–29535.
40 Shaul PW, Smart EJ, Robinson LJ, German Z, Yuhanna IS, Ying Y, et al. Acylation targets emdothelial nitric-oxide synthase to plasmalemmal caveolae. J Biol Chem. 1996;271:6518–6522.
41 Okamoto T, Schlegel A, Scherer PE, Lisanti MP. Caveolins, a family of scaffolding proteins for organizing “preassembled signaling complexes” at the plasma membrane. J Biol Chem. 1998;273:5419–5422.